

HERA Centroiding Image Processing Algorithm Based on the Normalised Correlation with a Lambertian Sphere

Stancu Florin Adrian¹, Marcos Avilés Rodrigálvarez², Andrea Pellacani², Ángel Palomino Aguado², Aída Alcalde Barahona², Francesco Pace², Paul Băjănaru¹, Víctor Manuel Moreno Villa² and Jesús Gil-Fernández³

¹GMV Innovating Solutions, SkyTower, 246C Calea Floreasca, Bucharest, Romania

²GMV Aerospace and Defence, Issac Newton 11, Tres Cantos, Spain

³ESTEC-ESA, Keplerlaan, Noordwijk, Netherlands

Keywords: Planetary Defence, Image Processing, Image Correlation, Visual Based Navigation, Guidance Navigation and Control.

Abstract: HERA is the spacecraft built by the European Space Agency (ESA) to visit and characterise the Didymos binary asteroid system after the impact performed by the NASA Double Asteroid Redirection Test (DART) mission. A visual-based Guidance Navigation and Control (GNC) system is developed for HERA to ensure safe ground, semi-autonomous and autonomous navigation around Didymos. For a better characterisation of the asteroids after DART post impact a close approach is foreseen. To ensure autonomous navigation during the close approach a visual-based GNC solution is developed by GMV, where dedicated image processing algorithms are implemented. Three main image processing algorithms are proposed to be used based on the distance of HERA spacecraft with respect to the Didymos system: normalised correlation with Lambertian sphere, centre of brightness with masking and feature tracking. This paper will briefly introduce the HERA mission and GNC, focusing more on the normalised correlation with a Lambertian sphere. Synthetic images generated based on Didymos (the main asteroid) and Dimorphos (the moon) are used for representative simulations. Performances are reported from a functional point of view until software (SW) implementation.

1 INTRODUCTION

HERA mission is the European component developed by ESA within the Asteroid Impact and Deflection Assessment mission, which is an international collaboration that materialised with the development of two spacecraft: DART and HERA. DART is the kinetic impactor launched in 2021 and it successfully impacted Dimorphos in September 2022. HERA is equipped with the necessary instruments to characterise asteroids and evaluate the crater generated by DART's impact. It will be launched in October 2024 and is expected to reach the Didymos system in January 2027. The Didymos binary system is composed of Didymos, the main asteroid, and Dimorphos, the moon of the system. HERA embarks several payloads, like the Image Processing Unit (IPU), Asteroid Framing Camera (AFC) and Juventas CubeSat. Juventas is a six-unit CubeSat designed to

operate in the close proximity of the Didymos system and take more risks. Similar to HERA, Juventas satellite is equipped with a visual-based navigation solution developed as well by GMV, with the objective to enhance navigation autonomy. A detailed description of Juventas' GNC architecture can be found in (Ovejero et al., 2023) and (Stancu et al., 2023).

HERA mission starts with the launch and early operation, where two launch windows have been identified in 2024 as the main date and a backup date in 2026. The next phase is the interplanetary transfer, where the HERA spacecraft is heading towards the Didymos binary system. The third phase is the rendezvous of HERA spacecraft with the Didymos system. The final stage is composed of multiple proximity operations: the early characterisation phase of the binary system, the payload deployment phase where the CubeSats are released, the detailed characterisation phase of the Didymos system, the

close operation phase near the asteroids, the experimental phase performing fly-bys and extended operation phase which will conclude with the end-of-life landing on Didymos.

The mission requires multiple levels of autonomy from semi-autonomous mode to autonomous navigation which can be obtained using a visual-based GNC system with dedicated image processing techniques feasible to be applied on asteroid shapes and surfaces. The visual-based GNC system allows HERA spacecraft to perform a close approach to Didymos in safe conditions in an autonomous manner. The autonomous operation is achieved through the translation navigation technology implemented inside the GNC systems. A navigation filter design based on an Extended Kalman is implemented and details can be found in (Palomino et al., 2023). The most important payloads contributing to this data fusion technique are the laser altimeter, the inertial measurement sensor, and the AFC acting like a pseudo-sensor (because the navigational information is extracted by the image processing algorithms). Three types of image processing technologies are implemented, which can be used in different scenarios: centroiding using normalised correlation with a Lambertian sphere, centre of brightness and feature tracking.

This paper focuses on the development of the HERA’s image processing technologies, providing in-depth details of the centroiding using normalised correlation with a Lambertian sphere algorithm. Considering ESA’s mission lifetime cycle definition, HERA is currently in phase D.

2 IMAGE PROCESSING TECHNOLOGIES ONBOARD HERA

The image processing approach is a key technology to ensure the close autonomous operation of HERA spacecraft near the Didymos system. The image processing algorithms are designed to use images in the visual spectrum. The first image processing algorithm is the centroiding using correlation with a Lambertian sphere (CLAMB). This technology can be applied only on Didymos, when the complete asteroid is in the camera’s field of view (FoV) and the range is as baseline higher than 9.5 km. The objective of the algorithm is to estimate the centre of Didymos in the image frame. In Figure 1 the CLAMB outputs are presented for one frame, in blue being represented the estimated centre and radius of Didymos.

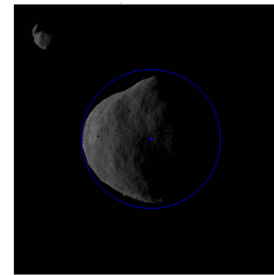


Figure 1: Robustness to Dimorphos presence in FoV.

The second technology is based on centre of brightness with masking and can be applied to both Didymos or Dimorphos. Masking is the process of removing the unwanted body from the image to avoid altering the centre of brightness position.

The last technology is based on feature tracking which detects and tracks features in consecutive images. The algorithm is based on the well-known Kanade Luca Tomasi feature tracker, adapted by GMV to fulfil functional and SW requirements of HERA spacecraft.

All three image processing algorithms are implemented directly in C and are wrapped under a single-entry point function called IP-SW. The HERA’s main onboard computer is a LEON3 processor which is a radiation-tolerant 32-bit processor. The IP-SW is scheduled to run on the second core of LEON3.

In Figure 2 the simplified architecture of the visual-based GNC is depicted, focusing on the general inputs/outputs and image processing chain. The GNC is implemented as a C application software (ASW) and together with the IP-SW form the visual-based GNC system.

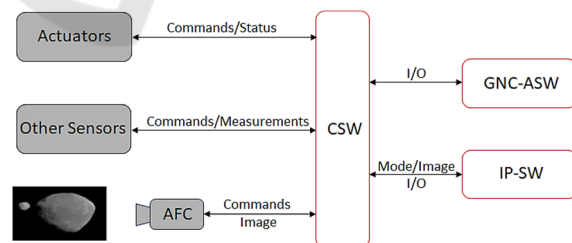


Figure 2: Simplified visual-based GNC system architecture.

The GNC-ASW and the IP-SW interact between them and with other components via the central software (CSW). The GNC-ASW is in charge of selecting which image processing algorithm is needed to run and ensure auxiliary inputs to IP-SW (for example the sun position). The image processing is extracting navigational information from the images, which is routed by CSW to GNC-ASW. The images

are obtained from AFC with a predefined periodicity defined by the proximity operation stage, with the scheduled requirement time of IP-SW execution up to a maximum of 48s.

For development and testing purposes a Functional Engineering Simulator (FES) was created from the beginning of HERA visual-based GNC system prototyping and maintained until phase D. The FES is integrating both the GNC and the image processing algorithms, but also models of real sensors or actuators. The images are generated by a synthetic image generator called PANGU. The FES is used to run extensive Monte Carlo (MC) simulations and to evaluate the fulfilment of requirements.

3 SYNTHETIC IMAGE GENERATION

The asteroids' shape and dimension are known from ground observations, knowledge that has been improved based on the scientific data acquired by the DART mission. To increase the representativeness of the vision-based GNC system validation and verification, the image processing algorithms are tested using synthetic image datasets. Nowadays, one of the most powerful synthetic image generators for space applications is the Planet and Asteroid Natural Scene Generation Utility (PANGU). PANGU is capable of creating high-resolution models of planets and asteroids, but also rendering images. Moreover, PANGU can integrate camera models and generate representative images given any position or orientation of the spacecraft, sun, planet or asteroid. PANGU is designed and validated for space image processing algorithms, therefore is natural to model and integrate the Didymos system scene in this application.



Figure 3: PANGU Didymos system, (Stancu et al., 2021).

Information about HERA Didymos reference model is provided in ESA-TECSP-AD-017258. The Didymos system is modelled starting from real data

and subsequently integrated into PANGU. The resolution of real models of the asteroids is artificially increased to comply with the image processing pixel ground sampling distance (GSD) needs.

It is important to note that a hyper-realistic generation of Didymos system implementation in PANGU was evaluated with good results from resemblance with a real asteroid, but finally it was discarded due to considerable computation time to initialise and generate images, in order of minutes per one image. This increased realism did not translate into any differences from the image processing algorithms' performance point of view.



Figure 4: Hyper-realistic PANGU Didymos in comparison with the Bennu asteroid.

The scene creation and the camera model, faithfully replicating the AFC characteristics, from Figure 2 are handled by PANGU. The most important configuration parameters of the AFC are: a FoV of 5.5 degrees, a sensor dimension of 1020x1020 pixels, a grayscale image in the visual spectrum, and a pixel depth for navigation images of 1 byte.

4 CENTROIDDING USING NORMALISED CORRELATION WITH A LAMBERTIAN SPHERE

The CLAMB objective is to determine the estimated geometric centre of Didymain in the image, thus providing to the navigation filter information about the Line of Sight (LoS) towards the centre of the asteroid. The proposed algorithm shall cope with at least the following scenarios: Dimorphos may appear in the image, Didymain has an irregular shape, various illumination conditions, Didymain and Dimorphos revolutions around their axis, defective pixels, high image background noise and photo response non-uniformity.

The following generic sequence of steps is performed, and later detailed in this chapter:

1. Image preprocessing.

2. Image binning, if necessary.
3. Estimate the rough angular size of Didymos from the image.
4. Correlate the image with different radiuses of Lambertian spheres.
5. Determine the sphere radius that maximises the normalised correlation.
6. Perform a correlation between the input image and the Lambertian sphere generated with the radius determined at point 5.

The image preprocessing is the initial correction step that prepares the images for further processing. The raw image can be affected by high background noise and photo response non-uniformity, but also by defective pixels. The background noise can be easily corrected by subtracting from the raw image the bias matrix, while the photo response non-uniformity is corrected by a multiplication gain matrix containing specific amplification factors for each pixel in part, as defined in equation (1). The gain and bias matrix are determined during the camera calibration procedure.

$$I_c = (I - B) \circ G \quad (1)$$

where $I^{m \times n}$ is the raw image from AFC of $m \times n$ dimension (padded with zeros until next power of 2 dimension), m represents the image number of rows, n represents the image number of columns, with the property that $m=n$, $I_c^{m \times n}$ is the corrected image, $B^{m \times n}$ is the bias matrix, $G^{m \times n}$ is the gain matrix and \circ denotes element-by-element matrix multiplication. Next, the defective pixel correction is performed based on a predefined list of bad pixels. A defective pixel can be either a hot or a cold pixel. The correction is performed for every bad pixel in part by considering the average of the pixel neighbourhood, using a median kernel.

A robustification method in the case of the presence of asteroid residue due to DART impact is currently being evaluated. A morphological opening operation is considered to remove small objects.

The image binning is useful to reduce the computation load on the processor, and it represents a downscaling of the image to reduce dimension. Eventually, I_c is defined to contain all the preprocessing, background noise and photo response non-uniformity correction, defective pixel correction, morphological opening and image binning.

The rough angular size of Didymos is estimated by counting the bright pixels in the image, which represents the area of Didymos seen in the image, A_{coarse} . To avoid considering possible artefacts present in the image, a bright pixel is defined to be a pixel with a value higher than a threshold. A multiplication phase angle factor is computed

because the asteroid could not be fully illuminated due to the sun phase angle, considering spacecraft-camera-sun geometry. Using the phase angle factor and the A_{coarse} the estimated area is corrected and is approximated with a circle to deduct the coarse radius in pixels, r_{coarse} . An additional measurement can be computed based on the r_{coarse} , namely the apparent range to Didymos, by knowing the Didymos real diameter in meters, the image dimension in pixels (considering a square image), and the camera's field of view.

The algorithm baseline is to correlate the image of Didymos with several radiuses of Lambertian spheres, thereby detecting the best correlation. The Lambertian spheres are generated starting from r_{coarse} by applying a multiplication factor. The multiplication factors can be detected automatically or can be set manually. The simulation shows that multiplication factors between $\pm 25\%$ from r_{coarse} are sufficient to detect the best correlations.

The generation of the Lambertian sphere is based on Lambert cosine law where the amount of light reaching on the surface of a body is computed based on the angle between the surface normal, N , and the light direction, L :

$$\cos(\theta) = \frac{N \cdot L}{\|N\| \cdot \|L\|} \quad (2)$$

The correlation is the technique proposed to determine the offset between two images and is based on the Fast Fourier Transform (FFT), which implies the transformation of the Didymos corrected image and Lambertian sphere image in the frequency domain.

The FFT correlation is performed as follows:

$$C_{FFT} = I_{cFFT} \square I_{modelLAMB} \quad (3)$$

where $I_{cFFT}^{m \times n}$ is the FFT transform of the Didymos pre-processed image, $I_{modelLAMB}^{m \times n}$ is the FFT transform of the Lambertian sphere model rotated 180 degrees, and \square represents the convolution operator which is a matrix multiplication element by element for complex numbers. The correlation will be repeated in a number of times equal to the Lambertian sphere candidates, defined by the multiplication factors.

To go back to the spatial domain, the inverse fast Fourier transform (IFFT) on C_{FFT} is applied, followed by an FFT shift to shift the zero-frequency components, finally obtaining the correlation $C^{m \times n}$. The 2-D fast Fourier transform is well covered in the scientific literature, however as a guideline, the reader can reference to the Matlab implementation of `fft2`, `ifft2` and `fftshift`.

At this point the correlation peak can be detected, its row and column position providing the estimated centre of Didymos. Because multiple Lambertian spheres are correlated to obtain the optimal radius, see Figure 6, the normalised correlation is proposed. The output of one correlation chain represents the row and column offset of Didymain, the peak normalised correlation value and the Lambertian sphere radius. Intuitively all this information will be obtained for all the Lambertian sphere candidates, which will further be used to determine the optimal radius that will maximise the correlation. Figure 5 depicts the correlation chain for one Lambertian sphere, preliminary results being available in terms of estimated asteroid centre and radius in the image frame, even though not optimal.

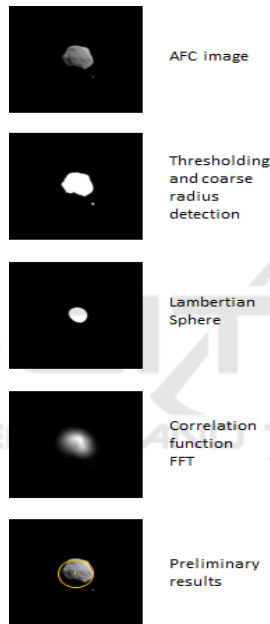


Figure 5: Correlation chain.

One final correlation is done for the sphere radius that maximises the correlation. The radius is determined based on information from previous correlations by fitting a quadratic function, equation (4), and selecting the best three Lambertian spheres that provide higher correlations. These correlations are noted in Figure 6, C_2 being the best correlation, C_1 and C_3 are C_2 left and right neighbours.

$$C_{quad} = ar^2 + br + c \quad (4)$$

where r is mapped as the radius and as C_{quad} the correlation.

By finding the best quadratic approximation the vertex can be found, C_v , and in consequence the best radius, r_{best} is:

$$r_{best} = -\frac{b}{2a} \quad (5)$$

Based on the r_{best} , a new Lambertian sphere is generated and correlated with the input image, to obtain the optimal estimation of the Didymain's centre in the image frame.

At this step, the estimated centre can be corrected for lens distortion, by using the Brown-Conrady model. It shall be noticed that specific polynomial coefficients are used, correcting the estimated centre from a distorted position to an undistorted position in the image frame.

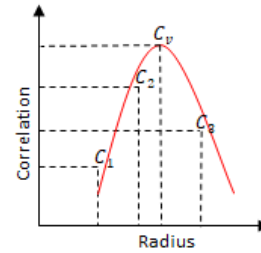


Figure 6: Quadratic approximation.

5 FPGA BASED IMAGE PROCESSING UNIT

The IPU is a GNC payload developed with direct applicability for the HERA mission. The unit is dedicated to the processing of the images taken by the AFC and it acts as an experimental aid for the on-board autonomous GNC.

The IPU provides isolation of image processing function and interfaces function, as it is relying on a two Field Programmable Gate Arrays (FPGA) architecture, with allocated external volatile and non-volatile memories. It includes one small and low-power consumption European FPGA: the rad-hard BRAVE NG-Medium, dedicated to interface control and monitoring, while the other one is a powerful FPGA that performs as a computer vision co-processor. The Processing FPGA is the high-density rad-hard Xilinx V5QV FPGA.

The SpaceWire interfaces allow telemetry and telecommand exchange between IPU and the on-board computer(s) via one nominal and one redundant SpaceWire links making use of the Packet Utilization Service (as per ECSS-E-ST-70-41-C). Alternatively, IPU can communicate with 2 separate instruments.

The two FPGAs included by IPU allow flexibility and many options for the design and implementation of complex functionalities, such as high-data rate interfaces management and hardware accelerators.

Different computer-vision accelerators which are not used in the same moment of time can be used during the mission by replacing bitstreams in the processing FPGA in-flight to save a potentially needed of second FPGA unit. The image processing techniques used by IPU – implemented in VHDL (and already stored before flight into the flash memory of the unit) are: CLAMB and feature tracking algorithm.

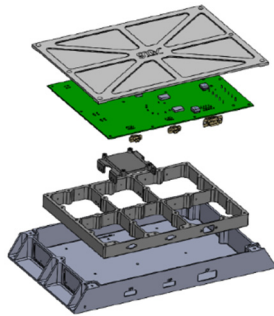


Figure 7: IPU exploded view.

The design, development and integration of the computer-vision algorithms for IPU are facilitated by the architectural design of the processing FPGA code, which provides an internal interfacing wrapper. IPU also includes pre-processing/correction functions for the image received from the navigation camera.

The development of the HERA IPU payload was incremental, including several models like: elegant breadboard, engineering model, engineering qualified model and flight model. The IPU has a total weight of 2.1 kg and it fits inside an envelope of 332 x 195 x 40 mm. Detailed information about IPU can be found in (Băjănaru et al., 2021).

6 FUNCTIONAL AND SW PERFORMANCES

To quantify the CLAMB performances, the experimental close fly-by scenario is considered, where all image processing technologies are used individually, by starting with CLAMB, then centre of brightness and ending with feature tracking. This analysis focuses on CLAMB taking advantage of the fact that the range varies considerably from approximately 20 km down to about 8.5 km. The FES plays a critical role in this analysis, using the real-world block to extract reference information that consists at least of spacecraft and Didymos attitude and position at each step of the simulation. The FES real-world data is used to compare the estimated measurement of CLAMB in terms of range, Didymos

centre and radius. The first metric to be evaluated is the apparent range estimation, represented in Figure 8 using an orange line, with respect to the real range of Didymos computed based on FES data, blue line.

From Figure 8, it can be noticed that a rough estimation of the range is obtained where Didymos shape uniformity has a direct impact on the stability of the metrics. The CLAMB estimated range is not used by the GNC but is a valuable input for the Fault Detection and Isolation system.

The following performances are derived for the estimated range and provided, in the form of mean range absolute error, standard deviation (STD) of the range absolute errors and the range relative mean error:

Table 1: CLAMB apparent range estimation performance.

Range absolute mean error [m]	Range absolute error STD [m]	Range relative mean error [%]
427.6	305.1	2.9

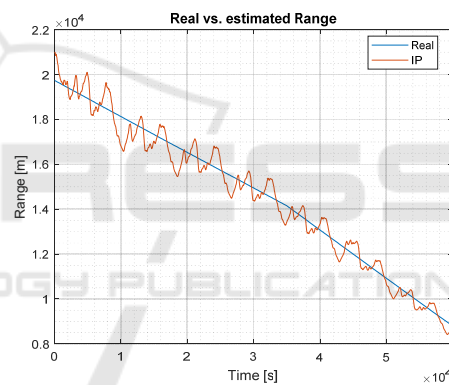


Figure 8: Real Didymos range vs CLAMB estimated range.

The CLAMB estimated centre in the image frame of Didymos is the most important output of the algorithm being directly used by GNC to maintain the asteroid inside the FoV.

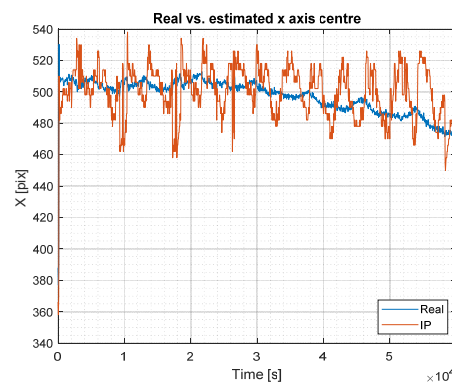


Figure 9: Real vs estimated centre on x axis.

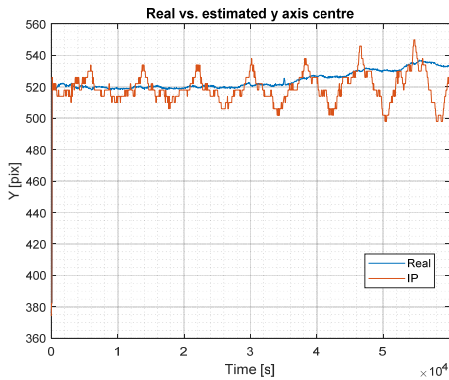


Figure 10: Real vs estimated centre on y axis.

The Figure 9 and Figure 10 present the performances on the x and the y axes, respectively, where the FES data is used to compute the reference centre of Didymos in the image frame for every image in part, blue line, with respect to CLAMB estimated centres, orange line. Top left corner image reference frame is used, x pointing to right and y pointing down. From Figure 9 and Figure 10, it can be observed that Didymos uniformity has a direct impact on the accuracy of the CLAMB centre estimation. This is a direct impact of the approximation with an ideal spherical shape when generating the Lambertian sphere. Another observation is the gradual error increasing in centre estimation caused by the close approach to Didymos, see Figure 8, and by the variation of sun phase angle starting from 90 deg at the beginning of the scenario and reaching almost 70 deg. However, the sun phase component error is very small due to the quadratic fitting optimisation procedure presented in equation (4).

The main component error is caused by the gradual approach to Didymos, thus reducing the range which affects the pixel GSD. The GSD is represented in meters, and is higher when the camera is further away from the surface that AFC is seeing, and lower when approaching the surface. Due to this phenomenon, the centre estimation error in meters remains almost constant.

Table 2: CLAMB centre estimation performance.

Axis	Centre absolute mean error [pix] / [m]		Centre absolute error STD [pix] / [m]	
x	13.4	18	9.9	13.5
y	7.6	9.5	7.3	7.6

In Figure 11 it can be noticed that the image is taken with initial knowledge of the spacecraft, moment of time when HERA’s AFC is not pointing towards the centre of Didymos. The CLAMB is able

to estimate the centre of the Didymos, blue star, which can be observed as well in the initial peak from Figure 9 and Figure 10. By making use of this measurement, the GNC is able to command HERA spacecraft and recursively maintain the asteroid in the centre of the image in the next frames.

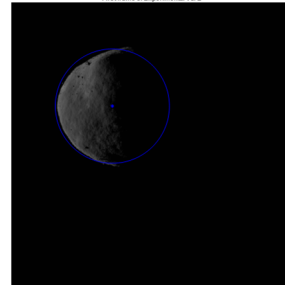


Figure 11: First frame close fly-by, blue star estimated centre, blue circle drawn based on estimated radius.

The optimised estimated radius presented in equation (5) can be considered as well as an output of CLAMB, see Figure 12.

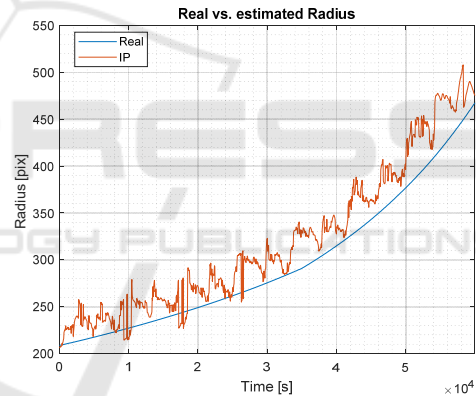


Figure 12: Real Didymos radius vs CLAMB estimated radius.

Similarly, based on FES data and AFC configuration the radius of Didymos asteroid can be approximated, blue line, and considered as a reference to compare the CLAMB estimated radius, orange line. The following performances are derived for the CLAMB radius estimation:

Table 3: CLAMB radius estimation performances.

Radius absolute mean error [pix]	Radius absolute error STD [pix]
24.83	14.33

From Figure 12, the presence of a constant bias can be observed, caused by the CLAMB correlation and radius optimisation procedure which tends to use

a Lambertian sphere radius that circumscribes Didymos. This is the reason behind the decision to use r_{coarse} to compute apparent range estimation.

As specified in section 2, the IP-SW wraps all the image processing under a single-entry point function, scheduled to run on the second core of LEON3. Taking into consideration that HERA is phase D, consolidated implementation requirements are imposed. The IP-SW is using less than 20 MB memory during runtime, excluding inputs/outputs and tuneable parameters. After SW optimisations performed by GMV the CLAMB implementation is using less than 3 MB of run-time memory. For the perspective of time execution, the TSIM-LEON3 emulator is used, set at 80 MHz. The execution time of CLAMB is determined for a subset of images using TSIM-LEON3. From Figure 13 the maximum execution time of CLAMB is up to 6.4 seconds during initialisation, mentioning that morphological opening is not included.

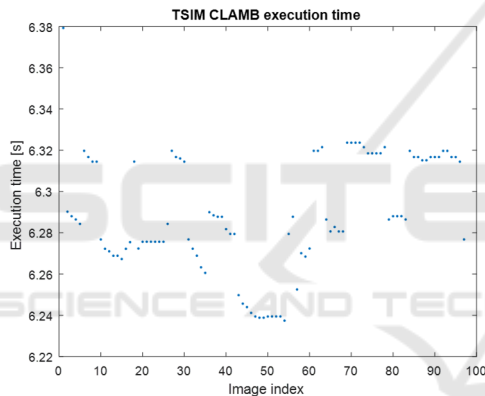


Figure 13: TSIM execution time.

7 CONCLUSIONS

This paper presents a detailed design of an image processing technique specific for asteroid centroid detection, that can be approximated with a spherical shape. The algorithm is based on the correlation with a Lambertian Sphere and is robust to various illumination conditions, Dimorphos appearance in FoV, and until a certain point robust to Didymos shape irregularity. The image processing algorithm offers the possibility to perform autonomous navigation around the Didymos binary system, thanks to the vision-based GNC system. The performances at pixel level are determined and reported for the range, centre and radius estimations of CLAMB. The IP-SW optimisation of CLAMB allows to run the SW in 6.4 seconds on a LEON3 processor. The CLAMB

algorithm was previously tested with success in a dedicated testing facility, **platform-art**®, where real mock-ups and camera were used, see (Pellacani et al., 2019). Extensive MC campaigns have been performed to test the visual-based GNC system, including the current baseline design of CLAMB and are reported in (Palomino et al., 2023).

ACKNOWLEDGEMENTS

The work presented in this paper is part of ESA HERA mission, expressing gratitude to the entire HERA mission team, particularly OHB as prime contractor and ESA as a client that has made possible the implementation of this mission and supported GMV through the whole process.

REFERENCES

- Băjănar, P., Domingo Torrijos, R., González-Arjona, D., Stancu, F. A., Onofrei, C., Marugan Borelli, M., Chamoso Rojo, R., Mihalache, C. G., (2021), Reconfigurable Co-Processor for Spacecraft Autonomous Navigation, In *2nd European Workshop on On-Board Data Processing (OBDP)*.
- Ovejero Provencio, D., Moreno Villa, V. M., Stancu, F., Plămădeală, A., Nistal Reñones, M., Domínguez Castillo, A. Plevier, C., Scoubeau, M., Cabral, F., (2023), The Juventas GNC Subsystem, Autonomous Landing on the Surface of the Binary Asteroid Dimorphos, In *ESA GNC and ICATT Conference 2023*.
- Palomino Aguado, Á., Pellacani, A., Cabral, F., Barahona A. A., Pace, F., Cortesse, A., Contreras Fernandes, R., Arribas Antonio, F., Stancu, F. A., Colmenarejo Matellano, P. (2023), Design, Development, Validation and Verification of the Hera GNC subsystem, In *ESA GNC and ICATT Conference 2023*.
- Pellacani, A., Graziano, M., Fittock M., Gil, J., Carnelli, I. (2019), HERA vision based GNC and autonomy, In *8th European Conference for Aeronautics and Space Sciences (EUCASS)*.
- Stancu, F. A., Moreno Villa, V. M., Domínguez Sánchez, C., Plămădeală, A. V., Ovejero Provencio, D., (2023), Visual based GNC system from prototype to flight software, In *INCAS Bulletin, Vol.15, Issue 1, pages 97-106*.
- Stancu, F. A., Garcia, J. R., Pellacani, A., González-Arjona, D., (2021), Validation process from model to HW avionics in the frame of HERA autonomous navigation, In *2nd Data System in Aerospace 2021 (DASIA)*.